Development of the electroweak phase transition and baryogenesis

Ariel Mégevand *
Centro Atómico Bariloche and Instituto Balseiro,
Comisión Nacional de Energía Atómica
and Universidad Nacional de Cuyo,
8400 San Carlos de Bariloche, Argentina

February 1, 2008

Abstract

We investigate the evolution of the electroweak phase transition, using a one-Higgs effective potential that can be regarded as an approximation for the Minimal Supersymmetric Standard Model. The phase transition occurs in a small interval around a temperature T_t below the critical one. We calculate this temperature as a function of the parameters of the potential and of a damping coefficient related to the viscosity of the plasma. The parameters that are relevant for baryogenesis, such as the velocity and thickness of the walls of bubbles and the value of the Higgs field inside them, change significantly in the range of temperatures where the first-order phase transition can occur. However, we find that in the likely interval for T_t there is no significant variation of these parameters. Furthermore, the temperature T_t is in general not far below the temperature at which bubbles begin to nucleate.

1 Introduction

The electroweak phase transition is an appealing scenario for the generation of the baryon asymmetry of the universe (BAU), since it contains the three

* megevand@cab.cnea.gov.ar

necessary ingredients known as Sakharov's conditions, namely, baryon number violation, C and CP violation, and a departure from thermal equilibrium. However, to obtain a quantitatively successful electroweak baryogenesis, one has to consider some extension of the Standard Model (SM) in which there is enough CP violation as well as a sufficiently strong first-order phase transition (see [1] for reviews). The order parameter used to measure the strength of the elecroweak phase transition is the mean value of the Higgs field in the broken symmetry phase at the critical temperature, $v\left(T_c\right) = \langle\phi\rangle_{T_c}$.

In the standard mechanism for electroweak baryogenesis, which assumes a first-order phase transition, the non-equilibrium condition acts in two different ways. The first of them is through the expansion of bubbles of the stable phase, which combined with CP violation inside the walls of bubbles produce non-equilibrium particle densities, which then give rise to the baryon asymmetry. The second effect of the departure from equilibrium is connected to the baryon number violation condition: baryon number violating processes must be turned off before the system reaches thermal equilibrium in order to avoid the washout of the generated BAU.

In the expansion of bubbles an asymmetry between left handed quarks and their antiparticles (and an opposite right handed asymmetry) is built up in front of the moving walls. This asymmetry biases the anomalous, baryon number violating sphaleron processes present in the high temperature phase. Thus, bubble walls must have a nonvanishing velocity to generate a net baryon asymmetry. On the other hand, the left-handed asymmetry injected in front of the wall needs some time to diffuse and bias the sphaleron processes before the reflected particles are re-caught by the wall. If the wall moves too fast, there won't be enough time for sphalerons to produce baryons. As a consequence, the generated baryon asymmetry has a peak at some small velocity which depends on the time scales associated to particle diffusion and baryon number violation [2, 3, 4]. In particular, it was shown in Ref. [4] that for the MSSM the peak is at $v_w = 0.01 - 0.03$.

The chiral quark asymmetry generated in front of the bubble wall depends also on the wall thickness. If the wall width is small compared to the inverse temperature, the CP-violating reflection of particles by the bubble wall can be treated quantum mechanically [5]. Otherwise, the effect of CP violation acts as a classical force on the quarks as they pass through the wall [6]. This is the case in the electroweak phase transition, since the wall width has been estimated to be $l_w \sim 10T^{-1}$ [7, 8, 9]. The final baryon asymmetry will thus also depend on l_w, resulting a larger asymmetry for thinner walls.

Regarding the avoiding of washout, sphaleron processes must be suppressed in the broken phase so that baryons that are created in front of the moving wall are not erased after entering the bubble. This requirement im-

poses a constraint on the sphaleron energy which can be expressed as the well known condition for the Higgs mean value [10]

$$\frac{v\left(T_c\right)}{T_c} \gtrsim 1 \ . \tag{1}$$

This condition gives a severe constraint for the theory of the electroweak interactions. Indeed, the minimal SM is unable to explain the observed BAU, since in this model the phase transition is not of the first order, but only a smooth crossover [11]. Furthermore, electroweak baryogenesis constrains the Minimal Supersymmetric Standard Model (MSSM) to a small region of parameter space, where the Higgs mass is less than about $105GeV$ and the stop mass is less than the top one [12, 7].

From the above it becomes apparent that phase transition dynamics plays a relevant role in electroweak baryogenesis. Being the baryon production very sensitive to the bubble wall width and velocity, and to the Higgs mean value, it is important to determine as accurately as possible the values of these parameters at the actual temperature of the phase transition. Indeed, all of these parameters vary significantly in the temperature interval in which the first-order phase transition can take place, that is to say, between the critical temperature T_c at which the two phases have the same free energy and the temperature T_0 at which the barrier between the two minima of free energy disappears. The exact temperature T_t of the transition depends on the evolution of the bubbles after they are nucleated, which in turn depends on the viscosity of the plasma.

In this paper we will analyze in detail the dependence on temperature of the parameters l_w, v_w, and $v\left(T\right)/T$, and we will determine the relative position of the temperature T_t in the interval $T_0 - T_c$. We will do this computation for different values of the parameters of our model, placing emphasis on those that adequate to the context of the MSSM. We will also discuss several aspects of the phase transition dynamics, such as transitory states in the evolution of the Higgs field, or the possibility that the transition occurs near the temperature T_0, where the mechanism of baryogenesis would be different from the usual one.

The plan is the following. In the next section we introduce our model for the first-order elecroweak phase transition, and calculate the shape of the nucleated bubbles as a function of temperature. In section 3 we study the subsequent evolution of the bubbles in the hot plasma. In section 4 we determine a temperature interval outside which the phase transition cannot occur, independently of the bubble evolution. Finally, in section 5 we compute the temperature and duration of the transition and discuss the implications for

baryogenesis. In the appendix we show some details of the numerical calculation.

2 The phase transition

The electroweak phase transition takes place when the expectation value of the Higgs field passes from its high temperature value $\langle\phi\rangle = 0$ to its nonzero value in the low temperature broken phase. We will use a simple model for the phase transition, which is nevertheless representative of the electroweak theory at high temperature.

2.1 The effective potential

We will assume that the free energy has the well known general form [8, 13, 14]

$$V(\phi, T) = D\left(T^2 - T_0^2\right)\phi^2 - ET\phi^3 + \lambda\phi^4 \ , \tag{2}$$

which will be suitable for our analysis, since it contains the essential features of the first order phase transition. Moreover, it can be a very good approximation to the actual effective potential. This is for instance the form of the perturbative high temperature effective potential in the SM [8, 13]. Even in the MSSM, which has two Higgs doublets, the free energy takes the SM-like form (2) in the limit in which the pseudoscalar particle of the Higgs sector is heavy ($m_A \gg T_c$) [14].

All the parameters in Eq. (2) depend on the particle content of the theory. Parameter D contains contributions from all the particles that acquire their masses through the Higgs mechanism. These contributions are of the form m_i^2/v^2, where m_i is the zero-temperature mass of particle i and v is the zero-temperature vacuum expectation value of the Higgs field. Parameter E has only boson contributions, of the form m_i^3/v^3. In the SM we have $D \sim 10^{-1}$, $E \sim 10^{-2}$, while in the MSSM, due to the larger particle zoo, D and E can be more than an order of magnitude larger than in the SM. Parameter λ is in general temperature dependent, but it is almost constant in the range of temperatures in which the phase transition can take place. This parameter is very sensitive to the Higgs mass and for our discussion we will assume it to be given parametrically by $m_H \sim \lambda v^2$.

The cubic term in $V(\phi, T)$ is responsible for the first-order feature of the phase transition, by causing the coexistence of two minima separated by a barrier. Hence, the strength of the transition depends on the value of parameter E. At high temperature the global minimum of the potential is

at $\phi = 0$. At the critical temperature

$$T_c = \frac{T_0}{\sqrt{1 - \frac{E^2}{\lambda D}}} \tag{3}$$

the two minima become degenerate, and below this temperature the stable minimum of V is at

$$v\left(T\right) = \frac{3ET}{2\lambda}\left(1 + \sqrt{1 - \frac{8}{9}\frac{\lambda D}{E^2}\left(1 - \frac{T_0^2}{T^2}\right)}\right) \ . \tag{4}$$

At temperature T_0 the barrier between minima disappears, and $\phi = 0$ becomes a maximum of the potential. The exact value of T_0 depends on the parameters of the theory, but we can assume it to be roughly $\sim 100GeV$ since the dynamics of the phase transition is not very sensitive to the value of this constant. The number $E^2/\lambda D$ is in general small, and the difference between T_c and T_0 is $\Delta T \lesssim 10^{-2} T_c$. However, as we shall see, things change rapidly as the temperature falls from T_c to T_0. Hence it proves useful to define a dimensionless variable

$$\varepsilon \equiv \frac{T_c^2 - T^2}{T_c^2 - T_0^2} \simeq \frac{T_c - T}{T_c - T_0} \ , \tag{5}$$

which goes from 0 to 1 as T runs between T_c and T_0.

At the critical temperature, Eq. (4) gives $v\left(T_c\right) = 2ET_c/\lambda$. Inserting this value into the condition for avoiding the washout of the baryon asymmetry [Eq. (1)], gives the constraint $\lambda \lesssim 2E$. In the SM this results in the bound on the Higgs mass $m_H \lesssim 40GeV$, well below the experimental bound $m_H^{\exp} \gtrsim 95GeV$. In the MSSM, the one loop stop contribution increases the value of parameter E, but this contribution is limited by the danger of inducing charge and color breaking minima. As a consequence, the bound on m_H can be shifted only to $\sim 80GeV$, provided that the light stop mass is in the range $100GeV \lesssim m_{\tilde{t}} \lesssim m_t$ [15]. It turns out that two loop corrections produce an enhancement of the strength of the phase transition, leading to an upper bound on the Higgs mass of $\sim 105GeV$ [12, 7].

Although Eq. (1) is written in terms of the critical temperature T_c, this condition is somewhat inexact, since at T_c the nucleation of bubbles has not yet begun. On the other hand, the phase transition must be completed when the temperature of the Universe is still above T_0, because bubbles of the true phase are copiously produced as the barrier between minima gets small and disappears. Hence, the transition takes place at an intermediate temperature $T_0 < T_t < T_c$ with

$$\frac{v\left(T_c\right)}{T_c} < \frac{v\left(T_t\right)}{T_t} < \frac{v\left(T_0\right)}{T_0} \ . \tag{6}$$

The temperature T_t is usually estimated by the condition $S_3(T_t)/T_t \sim 130 - 140$, where S_3 is the fluctuation in free energy which is necessary for bubble formation [8, 13, 14, 15, 16]. However, as was stressed in Ref. [13], a more careful determination of the temperature T_t is important, because the rate of anomalous baryon number violation is an exponentially sensitive function of $v(T)/T$. In the effective potential (2), $v(T)/T$ varies from $2E/\lambda$ at temperature T_c to $3E/\lambda$ at T_0. This variation by a factor of 3/2 gives an uncertainty of a 50% in the bound on the Higgs mass coming from Eq. (1). Elimination of this uncertainty is thus essential given the current experimental bounds on m_H. So the correct condition for avoiding the washout of the baryon asymmetry would be, according to Eq. (4),

$$\lambda < p(T) E \ , \tag{7}$$

where $p(T)$ is a number between 2 and 3, to be evaluated at the temperature of the phase transition, T_t.

2.2 Bubble nucleation

At a temperature below T_c, bubbles of the low temperature phase begin to nucleate. The thermal tunneling probability (per unit volume and time) for bubble nucleation is [17]

$$\Gamma \sim A(T) e^{-S_3/T} \ . \tag{8}$$

The prefactor $A(T)$ is roughly of order T^4 (so we will set $A(T) = T^4$), and $S_3(T)$ is the three-dimensional instanton action, which coincides with the free energy of the nucleated bubble. At high temperature the bounce solution is $O(3)$ symmetric, and the corresponding action takes the simple form

$$S_3 = 4\pi \int_0^\infty r^2 dr \left[\frac{1}{2} \left(\frac{d\phi}{dr} \right)^2 + V(\phi(r), T) \right] \ , \tag{9}$$

where $r^2 = \mathbf{x}^2$, and the equation for the configuration of the bubble is

$$\frac{d^2\phi}{dr^2} + \frac{2}{r}\frac{d\phi}{dr} = V'(\phi) \ , \tag{10}$$

with the boundary conditions $\phi(r = \infty) = 0$ and $\frac{d\phi}{dr}(r = 0) = 0$.

For temperatures close to T_c, the width of the bubble wall at the moment of formation is much smaller than its radius, and S_3 can be expressed as a function of the bubble radius r_0, the energy difference ΔV between the two minima of the potential, and the bubble wall surface energy σ [17]. The

radius of the critical bubble to be nucleated can thus be obtained by finding an extremum of $S_3(r_0)$. A similar approximation can be used to estimate the radius of a thick-walled bubble (i.e., outside the range of validity of the thin wall approximation) [13]. However, as was pointed out in Ref. [8], one must be very careful when evaluating S_3 in this way. Since the solution of Eq. (10) is a *maximum* of the action, the corresponding value of S_3 will be higher than the action of any approximate solution. As a consequence one can strongly overestimate the tunneling probability, leading to a sooner completion of the phase transition.

For the potential (2), Eq. (10) can be solved numerically and then integrated to obtain the action S_3, which can be expressed as a function of a dimensionless parameter $\alpha = \frac{\lambda D}{E^2}\left(\frac{T^2-T_0^2}{T^2}\right)$,

$$\frac{S_3}{T} = 13.72\frac{E}{\lambda^{3/2}}\ \alpha^{3/2} f(\alpha)\ . \tag{11}$$

Dine *et al.* [8] have found a useful analytical approximation to their numerical result for the function $f(\alpha)$,

$$f(\alpha) = 1 + \frac{\alpha}{4}\left(1 + \frac{2.4}{1-\alpha} + \frac{0.26}{(1-\alpha)^2}\right)\ , \tag{12}$$

with an accuracy of about 2% in the interval[1] $0 < \alpha < 1$. Using the same procedure we have calculated the radius r_0 of the nucleated bubble, the thickness l_w of its wall, and the value of the Higgs field inside it, ϕ_0, as functions of α. The calculation is described in the Appendix. Notice that the dimensionless function $p(T)$ defined by Eqs. (4) and (7) has also a simple expression as a function of α,

$$p(\alpha) = \frac{3}{2}\left(1 + \sqrt{1 - \frac{8}{9}\alpha}\right)\ . \tag{13}$$

Figure 1 illustrates the behavior of $r_0(\varepsilon)$ and $l_w(\varepsilon)$. Near the critical temperature ($\varepsilon = 0$) the bubbles that nucleate are thin-walled ($l_w \ll r_0$). This is because the energy difference between the two minima of the potential is much smaller than the energy barrier between them. In such a case the radius must be very large, so that the negative potential energy inside the volume of the bubble is able to compete with the positive surface energy. As ε increases, the wall width becomes of the same order of the radius and

[1]It is easy to see from Eq. (3) that $\alpha(Tc) = 1$, $\alpha(T_0) = 0$, and $\alpha \simeq 1 - \varepsilon$ in the whole interval.

the thin wall approximation breaks down. For $\varepsilon \to 1$ the size of the critical bubbles diverges. This is because the width of the bubble wall is associated to the correlation length, $l_w \sim \xi(T) \sim m(T)^{-1}$, with $m(T) = 2D(T^2 - T_0^2)$. This divergence is easily understood by looking at the shape of the bubbles. Figure 2 shows the bubble profile at a temperature near T_c ($\varepsilon = 0.1$), a temperature near T_0 ($\varepsilon = 0.9$), and at an intermediate temperature ($\varepsilon = 0.5$). Note that the value of the Higgs field inside the bubble decreases with ε. In

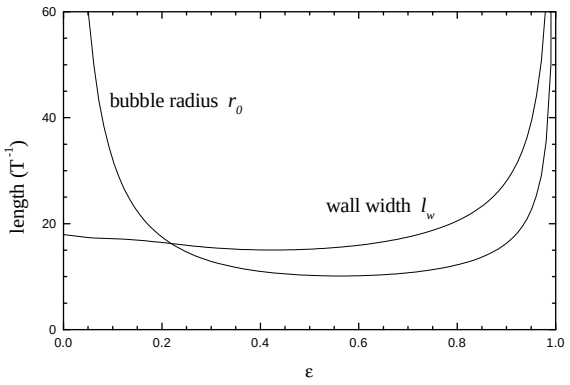

Figure 1: Bubble radius and wall thickness of the nucleated bubbles vs the relative messure of the temperature, ε, for $D = 1$, $E = 0.06$, and $\lambda = 2E$.

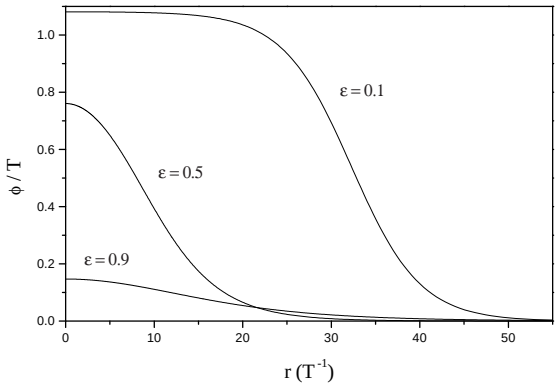

Figure 2: Shape of the critical bubble at different temperatures.

Fig. 3 we have plotted this value together with the minimum of the potential $v(T)$ for comparison. At $\varepsilon = 0$ the value of ϕ_0 coincides with that of $v(T_c)$. However, as the temperature decreases from the critical one, this value moves away from the minimum of $V(\phi)$ and goes to zero. This behavior is due the decreasing of the height of the barrier and the increasing in the energy difference between minima. In this case the value of $\phi(x)$ inside the bubble

needs not anymore to be exactly at the minimum of the potential to get enough volume energy. Moreover, as the barrier between minima disappears, it becomes easier to form a large bubble with a small value of ϕ inside it. Therefore, near the temperature T_0, bubbles with $r_0 \to \infty$ and $\phi_0 \to 0$ will be formed.

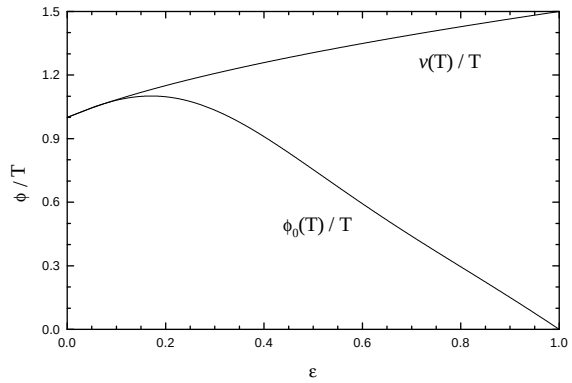

Figure 3: The minimum of the potential $v\,(T)$ and the value of ϕ inside the nucleated bubble, $\phi_0\,(T) \equiv \phi\,(r=0)$.

Consequently, if for any reason the transition does not occur until the temperature is close to T_0, then it will tend to proceed by a homogeneous growing of the order parameter ϕ, instead of by the nucleation and expansion of bubbles. This is not surprising since, without a barrier, one expects the field to "roll down" homogeneously towards the minimum of the effective potential [18]. There would still be some baryon number generation in such a scenario, due to the coherent variation of the CP violating field $\phi\,(t)$, which would produce an effective chemical potential for baryon number. However, this would be a kind of local baryogenesis [1] mechanism, and hence it would lack the enhancement due to diffusion, which characterizes the usual non-local electroweak baryogenesis. Furthermore, after rolling down the field will start to oscillate around the minimum of the potential until all its energy is transferred to the plasma. This oscillations can further spoil the generated baryon asymmetry, depending on their amplitude. This effect would be avoided in a phase transition at a higher scale, where the motion of ϕ would be strongly damped by the expansion of the Universe apart from the damping due to the plasma. Nevertheless, we shall see in section 4 that the phase transition is unlikely to occur beyond $\varepsilon = 0.5$, so the value of ϕ inside the bubbles at the moment of nucleation will not be far from $v\,(T)$.

We also see from Fig. 1 that the wall thickness is almost constant up to that value of ε, so we can anticipate that the width l_w, (which enters the

generated baryon number), will depend weakly on the temperature of the phase transition.

3 The evolution of bubbles

After a bubble is formed, it starts to grow due to the pressure difference between the phases separated by the bubble wall, $\Delta V = V(v,T) - V(0,T)$. After a short acceleration stage, the wall reaches a terminal velocity which depends on its interaction with the plasma. In this section we will analyze the evolution of bubbles from the moment they are nucleated until they fill the Universe

3.1 Bubble wall propagation

If the time it takes a bubble wall to accelerate up to terminal velocity is much smaller than the time it propagates before colliding with other bubbles, then the initial acceleration stage can be ignored. In order to check that this is the case, we can estimate the time needed for the wall to reach terminal velocity from the equation of motion for ϕ in the plasma, Eq. (17) below. If the field is strongly damped the wall will reach terminal velocity faster than without damping, so using Eq. (17) without the damping term one can estimate the maximum acceleration time [3]. In such a case the wall reaches the speed of light in a time $\tau \sim v(T)^2 / (l_w V(v(T),T))$. For the values of the parameters of $V(\phi,T)$ that we will consider, this gives $\tau \sim (10^2 - 10^4)\, T^{-1}$.

In order to compare this time with the typical times associated with the phase transition, we need the relation between the temperature of the Universe and time. At the radiation-dominated era it is given by

$$t = \frac{\xi M_{Pl}}{T^2} \ , \tag{14}$$

where $M_{Pl} = 1.22 \times 10^{19} GeV$ is the Plank mass, and ξ is a factor that depends on the effective degrees of freedom of the plasma. Near the temperature of the electroweak phase transition, $\xi \simeq 1/34$. The time elapsed between T_c and T_0, for instance, is

$$\Delta t_{T_c - T_0} \sim \frac{\xi M_{Pl}}{T_c} \frac{T_c - T_0}{T_c} T_c^{-1} \sim 10^{13} T^{-1} \ , \tag{15}$$

which is many orders of magnitude larger than τ. However, to check if the short acceleration assumption is correct we must compare τ with the time in which a typical bubble propagates until all space is filled by broken symmetry

bubbles. This time is of the order of the duration of the phase transition Δt_t, which is less than $\Delta t_{T_c - T_0}$. We will see in section 5 that $\Delta T_t \simeq 10^{-3} (T_c - T_0)$, so $\Delta t_t \sim 10^{10} T^{-1}$. The assumption is thus valid.

There is another transitory stage, associated with the growing of ϕ in the interior of the bubble. As seen in Fig. 3, bubbles nucleate with a value of the field inside them, $\phi_0 (T)$, that is less than that of the minimum of the potential $v(T)$. This fact can be important for the bubble wall propagation, since the pressure difference $V(\phi_0, T) - V(0, T)$ that pushes the wall would then be less than $V(v, T) - V(0, T)$. Again, we can use Eq. (17), this time discarding all spatial derivatives, to calculate the time in which $\phi(r = 0)$ grows from ϕ_0 to v. Neglecting the damping term we obtain $\tau \sim \sqrt{\Delta\phi / V'(\phi)}$. For $\Delta\phi \simeq \phi_0 \simeq v/2$ this gives $\tau \sim 10 T^{-1}$. With a damping term it will take the field a longer time to get to v. Assuming a typical damping $\eta \sim 100$ (see below), we obtain $\tau \sim \Delta\phi \eta / V'(\phi) \sim (10^4 - 10^5) T^{-1}$, which is again much less than Δt_t.

We can therefore safely assume that $\phi(r = 0) = v(T)$, and that bubble walls move with constant velocity through the plasma. The friction on the bubble wall depends on the departure from equilibrium of the particle distributions near the wall [8, 19, 20]. Particles which interact with the Higgs field in such a way that their masses change across the bubble wall profile will feel a force as they are caught by the propagating wall. Integration of these forces weighted with the particle distributions gives the total force exerted on the wall by the plasma. When equilibrium distributions appropriate for the local value of ϕ are considered, this force only accounts for the finite temperature part of ΔV, and does not depend on the wall velocity. Nevertheless, a departure from equilibrium is in fact produced by the motion of the wall. Particles that, for energetic reasons, cannot penetrate the wall, are reflected in front of it. These particles slow down the wall by giving momentum to it, and this effect becomes more important the faster the wall moves. Expanding the non-equilibrium particle distributions to first order in the wall velocity, the force gets a contribution proportional to the wall velocity [8]. The terminal velocity is thus obtained by equating this frictional force with ΔV.

The propagation of the bubble wall can also be affected by hydrodynamics (see for instance [3, 21, 22]). Although hydrodynamic considerations are important for large velocities, if the wall velocity is small the only important effect is a global reheating due to the latent heat released by the expanding bubbles [3]. Indeed, when the velocity of the bubble wall is less than the speed of sound in the relativistic plasma $c_s = \sqrt{1/3}$, it propagates as a deflagration front. This means that a shock front precedes the wall, with a velocity $v_{sh} > c_s$. Hence, the latent heat is transmitted away from the wall. If the wall velocity is small enough, the latent heat has time to distribute

throughout space, causing a homogeneous reheating of the plasma as the wall propagates.

There exist other effects that can influence the growth of bubbles. An example is that of strong magnetic fields that can be formed before [23] or during [24] the electroweak phase transition. The presence of these fields changes the free energy difference between phases, thus affecting the temperature and strength of the first order phase transition [25]. In the case that the magnetic fields are generated during the electroweak phase transition, they can delay the completion of the latter by strongly affecting the evolution of bubbles [18].

3.2 The wall velocity

The equation of motion for the bubble wall in the hot plasma can be derived by energy conservation considerations [8, 19, 20] ,

$$\partial_\mu \partial^\mu \phi + \frac{\partial V(\phi, T)}{\partial \phi} + \sum_i \frac{\partial m_i^2}{\partial \phi} \int \frac{d^3p}{(2\pi)^3 2E_i} \delta f_i = 0 \ , \tag{16}$$

where δf_i is the deviation from the equilibrium distribution function for particle species i in the heat bath. The last term can be expressed [3, 21] as a frictional damping term proportional to $d\phi/dt$. Due to Lorentz invariance this term must be of the form $u^\mu \partial_\mu \phi$, where u_μ is the four-velocity of the plasma. Eq. (16) then becomes

$$\partial_\mu \partial^\mu \phi + V'(\phi) + (\eta T)\, u^\mu \partial_\mu \phi = 0 \ , \tag{17}$$

where η is a dimensionless damping coefficient that depends on the viscosity of the medium, and is obtained by calculating the deviations δf_i near the wall.

The calculation of the friction is usually treated with kinetic theory [8, 19, 20], giving for the Standard Model roughly $\eta \sim 1$. However, it was noticed [26] that infrared boson excitations which are treated classically [27], increase the value of η by an order of magnitude. In the MSSM there is an additional enhancement of the friction due to the larger particle content of the model. In Ref. [28] the contribution of a light right-handed stop has been calculated, which added to the contributions of tops and W bosons give a lower bound on the friction coefficient of $\eta \simeq 70$.

We will not take into account other effects such as the influence of magnetic fields on the bubble growth. Instead, we will consider values of the friction beyond $\eta \sim 100$ to allow for the possibility of additional damping,

and we will assume that that kind of effects can be parametrized in this way. Accordingly, we will let η vary in the range $1 < \eta < 1000$.

The nucleated bubbles grow rapidly to a size large enough so that we can go to 1+1 dimensions. Boosting to a frame that moves with the wall and assuming stationary motion in the x direction we then have

$$\frac{d^2\phi}{dx^2} = V'(\phi) - \eta T v_w \gamma \frac{d\phi}{dx} \ , \tag{18}$$

where $\gamma = 1/\sqrt{1-v^2}$. Multiplying both sides by $d\phi/dx$ and integrating over $-\infty < x < \infty$, we obtain a formula for the wall velocity,

$$v_w \gamma = \frac{1}{\eta T} \frac{\Delta V}{\sigma} \ , \tag{19}$$

where $\Delta V(T)$ is the free energy difference between the two phases and $\sigma(T)$ is the surface tension of the wall,

$$\sigma(T) = \int_{-\infty}^{+\infty} \left(\frac{d\phi}{dx}\right)^2 dx \ . \tag{20}$$

We have assumed here that temperature is constant across the wall. This is right if the wall velocity is small enough that the latent heat it releases has time to be uniformly distributed throughout space [3]. If we use the well known kink approximation for the wall profile (see for instance [30])

$$\phi(x) = \frac{v(T)}{2}\left[1 + \tanh\left(\frac{x}{l_w}\right)\right] \ , \tag{21}$$

then the surface energy (20) is $\sigma = v^2/3l_w$, and the wall velocity is given by

$$v_w \gamma = \frac{3 l_w \Delta V}{T \eta v^2} \ . \tag{22}$$

We see from Eq. (22) that v_w increases with l_w. This is because the thicker the bubble wall, the slower will be the variation of ϕ as the wall sweeps through a given point in the plasma, and consequently, the smaller the disturbance of the plasma near the wall. Hence, thicker walls experience a smaller friction force from the medium. Since l_w diverges at T_0, one can infer that the dependence of the velocity with the wall width gives an important variation of v_w with temperature. In the literature, however, l_w is usually evaluated near the critical temperature. For instance, it is often roughly approximated by the correlation length $m(T_c)^{-1}$ [3, 26], or it is taken from the wall profile at the temperature at which $S_3(T)/T \sim 130-140$ [7, 8, 9, 28].

This gives $l_w \sim (10-40)\,T^{-1}$ for the electroweak bubble. We can see from Fig. 1 that these approximations are good as long as the phase transition completes before the temperature gets close to T_0, since l_w is almost constant until $\varepsilon \simeq 0.8$. As we will see in the next section, the phase transition hardly occurs beyond that value of ε.

Figure 4 shows the terminal velocity of the bubble wall as a function of ε. In the interval $0 < \varepsilon < 1$ it varies from $v_w = 0$ (since $\Delta V = 0$ at the critical temperature) to $v_w = 1$ (since $l_w \to \infty$ for $\varepsilon \to 1$). Note, however, that at the beginning of the interval the wall velocity grows rapidly from 0 to some value proportional to η^{-1}, then it becomes rather insensitive to ε, and finally it grows again up to $v_w = 1$. As we shall see, the electroweak phase transition generally occurs at some intermediate ε so, for fixed η, the wall velocity will not be very sensitive to the temperature of the transition.

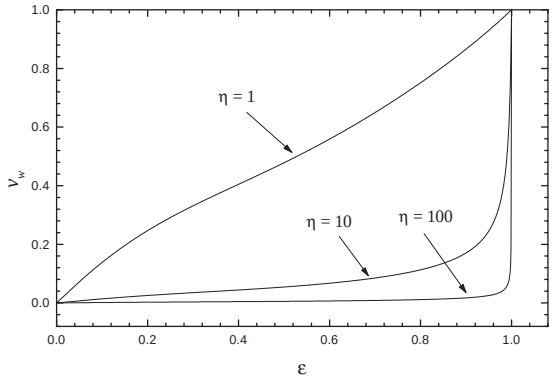

Figure 4: Bubble wall velocity as a function of ε, for three different values of the damping coefficient η.

3.3 Fraction of space occupied by bubbles

Once a bubble has nucleated, its wall rapidly reaches the terminal velocity v_w, which depends on temperature. Due to the large time-temperature relationship (14), v_w varies slowly with time, so the evolution of the bubble radius can be approximated by

$$r\left(t', t\right) = r_0\left(t'\right) + v_w\left(t'\right)\left(t - t'\right) \tag{23}$$

where $r_0\left(t'\right)$ is the radius of the bubble at the moment t' of its formation[2]. The number of bubbles created per unit volume between t' and $t' + dt'$

[2]By the epoch of the electroweak phase transition, the variation of length scales due to the expansion of the Universe can be neglected during the short period between T_c and T_0.

is $dn_b(t') = \Gamma(t')\,dt'$. Then at time t the total volume of bubbles that have nucleated at previous times $t_c < t' < t$ is (per unit volume of space) $\int_{t_c}^{t} \Gamma(t')\,(4\pi/3)\,r(t',t)^3\,dt'$. This formula, however, contains multiple counting of volume where bubbles overlap. A more exact expression was obtained in Ref. [29] for the fraction of space $f(t)$ that is still in the false vacuum,

$$f(t) = \exp\left\{-\frac{4\pi}{3}\int_{t_c}^{t}\Gamma(t')\left[r_0(t') + v_w(t')\,(t-t')\right]^3 dt'\right\} \ . \qquad (24)$$

The phase transition then completes when $f(t)$ falls to zero. All the quantities appearing in the integral are in fact functions of temperature, so the use of the time-temperature relation (14) will be needed in the computation.

Some reheating will occur at the end of the transition due to collisions of bubble walls. However, for small wall velocities this effect should not be important. As we have already mentioned, the main consequence of the release of energy by slowly-expanding bubbles is a global reheating *during* the bubble expansion stage, which would manifest itself by changing the time-temperature relation. Taking into account this effect would require solving the two coupled equations for $T(t)$ and $f(t)$, which is outside the scope of the present paper. Before going on, however, we would like to discuss the relevance of such an effect. As pointed out in Ref. [3], one can get an idea of how important the reheating is by comparing the latent heat

$$L \equiv T\frac{\partial V(\phi,T)}{\partial T}\bigg|_{v,T_c} = 8\frac{DE^2}{\lambda^2}T_0^4 \qquad (25)$$

with the energy needed to bring the plasma back up to T_c from T_t,

$$\rho(T_c) - \rho(T_t) = a\left(T_c^4 - T_t^4\right) \ , \qquad (26)$$

where the factor a depends on the number of effectively massless degrees of freedom. At the time of the electroweak phase transition $a \simeq 35$. Since $T_c - T_t \lesssim T_c - T_0$, the energy density difference will be $\Delta\rho \lesssim T_c^4$. For SM values of D and E, the latent heat is smaller than $\Delta\rho$ by one or two orders of magnitude, depending on the value of λ. For MSSM values of the parameters, instead, L can be of the same order of magnitude of $\Delta\rho$. In such a case the latent heat released by the bubbles could reheat the plasma back up to temperatures near T_c. So we must remark that this effect might be important for baryogenesis. Due to the small velocity of the bubble walls, the gradually released latent heat will prevent the temperature of the bath to decrease, rather than reheating the plasma at the end of the transition. If the temperature stays close to T_c, the pressure difference ΔV across the bubble walls will be small, and hence the wall velocity can decrease considerably from the current estimations [3].

4 The temperature of the phase transition

The progress of the phase transition is determined by the fraction of space $f(T)$ that is still in the symmetric phase, given by Eq. (24). In the next section we will calculate the temperature T_t of the transition and its duration ΔT_t for different values of the friction. However, since the exact evolution of the bubble wall velocity is not known, it will be convenient to begin our analysis by putting reliable constraints on T_t inside the interval $T_0 - T_c$.

We will consider two sets of values for the parameters E and D of the potential: those corresponding to the SM, $E \simeq 6 \times 10^{-3}$, $D \simeq 0.2$; and MSSM-like values, which for definiteness we set $E \simeq 6 \times 10^{-2}$, $D \simeq 1$. In both cases we will take $\lambda/E = 2$ or 3, which correspond respectively to $v(T_c)/T_c = 1$ or $v(T_0)/T_0 = 1$. Although the SM with these values of the parameters is not a realistic model, for the sake of comparison it is useful to consider such a kind of parameters besides those corresponding to the MSSM, in order to simulate a different phase transition with the same simple form of the effective potential. Regarding the MSSM-like values, it is worthy to remind that our model Eq. (2) corresponds to the limit of only one light Higgs boson of the MSSM, and the values of the parameters correspond to the light right-handed stop scenario.

4.1 An upper bound

The temperature T_N at which nucleation of bubbles begins is defined as that at which the first bubble is formed inside a causal volume [13]. In the radiation dominated era the horizon size scales like $d_H = 2t$, where the age of the Universe t is given by Eq. (14). Hence the size of a causal volume is $V_H \sim 8\xi^3 M_{Pl}^3/T^6$, and the probability of nucleating a bubble inside it is

$$P(T) = \int_{t_c}^{t} \Gamma V_H dt = (2\xi M_{Pl})^4 \int_{T_c}^{T} e^{-S_3/T} \frac{dT}{T^5} \, , \tag{27}$$

where we have used Eqs. (8) and (14) in the last step. The temperature T_N is thus determined by the condition $P(T_N) \sim 1$. This can be solved either by an analytical approximation [13] or numerically, and gives

$$S_3(T_N)/T_N \simeq 135 \, . \tag{28}$$

Although T_N is often assumed to be the temperature of the transition, it only corresponds to the onset of nucleation, so it gives an upper bound for T_t.

Once bubbles begin to nucleate, however, it still takes them some time to fill all space, since bubble walls cannot move faster than light. A less conservative bound $T_{\max} < T_N$ can thus be obtained by setting $v_w = 1$ instead of using Eq.(22) for v_w in Eq. (24). In this limit the expansion of bubbles is so fast that we can neglect their initial radius r_0. Then the condition that the fraction $f(T)$ falls to zero can be expressed as

$$\frac{4\pi}{3}\left(2\xi M_{Pl}\right)^4 \int_T^{T_c} e^{-S_3(T')/T'} \left(T'-T\right)^3 \frac{dT'}{T'^5} \sim 1 \ , \tag{29}$$

giving for the upper bound $T_{\max}$

$$S_3\left(T_{\max}\right)/T_{\max} \simeq 105 - 109. \tag{30}$$

The small uncertainty is due to the variation of the parameters of the potential as we take SM-like or MSSM-like values and the ratio λ/E in the range $2-3$.

4.2 A lower bound

It is easy to see from Eqs. (11) and (12) that the instanton action S_3 vanishes at T_0. Hence, there is no exponential suppression to the nucleation rate Γ at that temperature (this is a consequence of the disappearance of the barrier of $V(\phi)$ at T_0). At temperatures near T_0 the nucleation rate is thus $\Gamma \sim T^4$, which is extremely large. Indeed, $\Gamma = T^4$ means that in a time interval $\tau \sim T^{-1}$ a bubble forms in every volume $\mathcal{V} \sim T^{-3}$. This time τ is many orders of magnitude less than the time elapsed between T_c and T_0, Eq. (15). In addition, the size of the nucleated bubbles is larger than the volume per bubble $\mathcal{V}$, since the radius of the electroweak bubble is always larger than a few T^{-1}. So all space must be filled with bubbles before the Universe cools down to some temperature $T_{\min} > T_0$, when the exponential factor in Eq. (8) is still much less than 1.

We can calculate the lower bound $T_{\min}$ by setting $v_w = 0$ in Eq. (24),

$$\frac{8\pi\xi M_{Pl}}{3} \int_{T_{\min}}^{T_c} \Gamma(T)\, r_0^3(T)\, \frac{dT}{T^3} \sim 1 \ . \tag{31}$$

This corresponds to the (unrealistic) limit of a nucleation-dominated first-order phase transition. The opposite limit is that of a bubble expansion dominated phase transition, in which the nucleated bubbles grow so rapidly that the original size is negligible, and the transition is completed when the nucleation rate is still small [13]. This is the case of the upper bound $T_{\max}$ we

have just estimated. As we shall see, the electroweak phase transition is closer to an expansion dominated transition than to a nucleation dominated one. The temperature $T_{\min}$ determined by Eq. (31) is given by $S_3\left(T_{\min}\right)/T_{\min} \simeq 35 - 38$.

In terms of the relative variable ε, the bounds on the temperature of the transition are expressed as $0.31 \lesssim \varepsilon_t \lesssim 0.52$ for SM values of E and D, and $0.15 \lesssim \varepsilon_t \lesssim 0.31$ for MSSM values of the parameters (setting for definiteness $\lambda = 2E$ in both cases).

5 Numerical results

In the last section we have determined the temperatures $T_{\max}$ and $T_{\min}$ between which the phase transition takes place. Depending on the value of the friction parameter η, the temperature of the phase transition will be closer to one of these bounds.

5.1 The development of the phase transition

The fraction of space that is still in the symmetric phase is obtained by inserting Eq. (22) into Eq. (24) and solving numerically for $f\left(T\right)$. We have plotted $f\left(\varepsilon\right)$ in Fig. 5 for a given choice of parameters, in order to illustrate the evolution of the phase transition. Note that, once the fraction of volume occupied by bubbles becomes appreciable, the phase transition completes in a tiny temperature interval. That is why we speak of the "temperature of the transition" rather than of a "temperature interval". No relevant quantity will change appreciably in this interval. This is due to the large time-temperature relation, which governs the nucleation and expansion of bubbles. The duration of the phase transition varies very little with the friction. It is given by

$$\frac{\Delta T_t}{T_c - T_0} \simeq \Delta\varepsilon_t \simeq 5 \times 10^{-3} \tag{32}$$

for values of η as large as 10^5 as well as for no friction at all.

With no friction, the phase transition occurs at $T_{\max}$. When friction is turned on, the transition is retarded, as shown in Fig. 6. Note that the dependence of ε_t with η is almost logarithmic, so ε_t increases more slowly for large η. As a consequence, T_t will be closer to $T_{\max}$ rather than to $T_{\min}$ for not extremely high values of η. As discussed in section 3, η should not be out of the range $1 - 1000$.

In Fig. 7 we have plotted the value of S_3/T at the moment of the transition, as a function of the damping coefficient. The solid line corresponds to

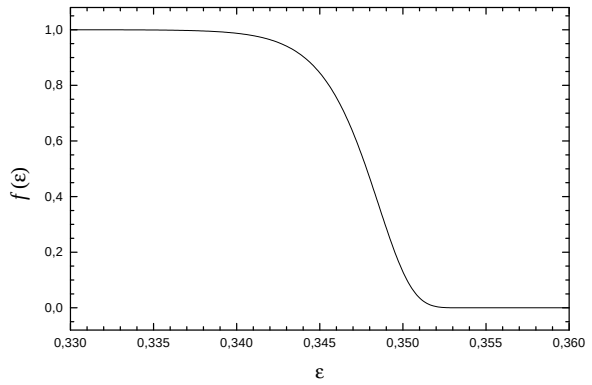

Figure 5: Fraction of space in false vacuum as a function of ε, for $\eta = 100$, $D = 0.2$, $E = 0.006$ and $\lambda = 2E$.

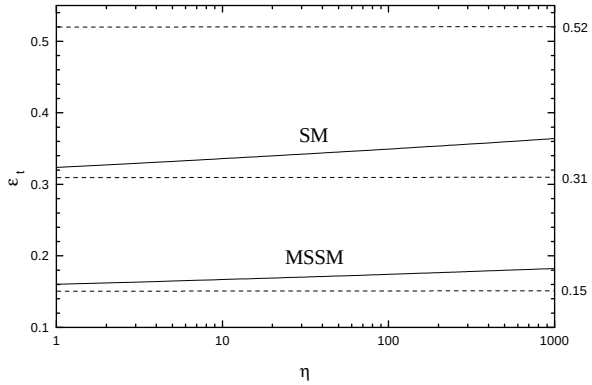

Figure 6: The temperature of the transition as a function of the friction η. The upper curve corresponds $D = 0.2$, $E = 6 \times 10^{-3}$, and $\lambda = 2E$. The lower one is for $D = 1$, $E = 6 \times 10^{-2}$. The temperatures corresponding to upper and lower bounds are indicated with dashed lines.

MSSM values of the parameters. For likely values of the friction, $\eta \sim 100$, the temperature of the transition is given by $S_3(T_t)/T_t \simeq 90$. The dashed line indicates the variation in S_3/T when considering different parameters of the effective potential, as explained in the previous section. Since the ambiguity in $S_3(T_t)/T_t$ produced by such a variation is of only a 5%, we believe that Fig. 7 not only describes qualitatively the general case, but it would also give a good approximation for the determination of the temperature of the electroweak phase transition within different models.

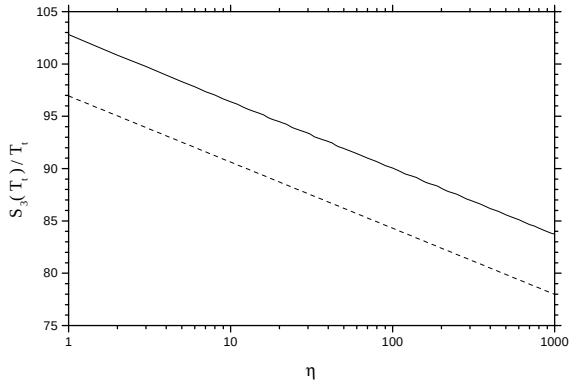

Figure 7: The value of the three dimensional action S_3 at the temperature of the transition, for $D = 1$, $E = 0.06$ and $\lambda = 2E$. The dashed line shows the maximum shift of the curve as D, E and λ are varied as indicated in Sec. 4.

5.2 Implications for baryogenesis

The amount of baryon number generated at the electroweak phase transition depends on the shape of bubbles. We have seen that the relevant parameters, namely, the width and velocity of the bubble wall and the value of the Higgs field in the broken symmetry phase, vary significantly between the temperatures T_c and T_0, and hence the importance of determining their values at the intermediate temperature T_t at which the phase transition occurs.

Regarding the wall velocity, we have shown in section 3 that, although v_w takes all the possible values $0 < v_w < 1$ in the interval $0 < \varepsilon < 1$, it changes rapidly at the beginning and at the end of that interval, but remains of the same order of magnitude for intermediate values of ε, roughly between $\varepsilon = 0.1$ and $\varepsilon = 0.8$ (see Fig. 4). Since the bounds on T_t obtained in section 4 fall in this region of slow variation of v_w, we see that the wall velocity depends weakly on the actual temperature of the transition, although it is sensitive to the friction, as shown in Fig. 4. Therefore, rough approximations of the temperature of the transition, such as the usual $T_t \simeq T_N$, do not introduce significant errors in the estimation of v_w. The same can be said of the wall thickness, as inferred from Fig. 1.

Typical values of these quantities are found by taking for instance $\eta = 70$ and MSSM-like parameters for ΔV. Then we obtain $l_w(T_t) \simeq 16T^{-1}$, which inserted into Eq. (22) gives $v_w(T_t) \simeq 3 \times 10^{-3}$. This is in agreement with the value obtained in Ref. [28], and supports an MSSM scenario for electroweak baryogenesis.

With respect to the Higgs mean value $v(T)$, although it varies by a 50% between T_c and T_0, the variation between the critical temperature and T_t

will be smaller. As shown in Fig 6, the temperature of the transition stays close to the upper bound (lower bound on ε_t), even for large values of η. We can use Eq. (13) to estimate by which amount the order parameter can change. Setting for definiteness $\lambda = 2E$, like in Fig. 6, we see that for $\eta \sim 100$ the upper curve in the figure gives $\varepsilon_t \simeq 0.35$. Since $v(T)/T = (E/\lambda)\, p(\alpha)$ and $\alpha \simeq 1 - \varepsilon$, we readily obtain $v(T_t)/T_t \gtrsim 1.2$. Similarly, for the lower curve we obtain $v(T_t)/T_t \gtrsim 1.1$. Comparing with $v(T_c)/T_c = 1$, we find a difference of at least a $10 - 20\%$ between the critical temperature and the actual temperature of the transition. This means that the use of Eq. (1) can result in an upper bound on the Higgs mass that is by that percentage more severe than the correct constraint. A more precise bound for λ can be obtained by using Eq. (7) recursively. For instance, after computing ε_t with the assumption $\lambda = 2E$ and calculating the constraint $\lambda = p(\varepsilon_t)\, E$, this new value of λ can be used to recalculate ε_t and obtain a higher order correction to the bound. This may be useful when considering a more concrete model for the phase transition.

The error in the determination of $v(T_t)/T_t$ diminishes considerably when using the temperature T_N of the onset of nucleation instead of T_c. For the values of the parameters that we have considered, $v(T)/T$ increases by less than a 5% between T_N and T_t. Hence, regarding the constraints that result by avoiding the washout of the baryon asymmetry, we again find that $T_t \simeq T_N$ is a good approximation in the calculations of electroweak baryogenesis.

Before concluding, we would like to discuss the behavior of another bubble parameter that is relevant for baryogenesis in the MSSM, that is, the relative variation of the two Higgs fields across the wall, $\Delta\beta$. The CP-violating force on the quarks depends on this variation, and thus the final baryon asymmetry results proportional to $\Delta\beta$. In order to investigate the temperature dependence of this parameter, however, we would need to consider the full two-Higgs model. The computation of the bubble profile with more than one scalar field is a difficult task (see for instance [9, 30]). Nevertheless, our results for the temperature of the transition can be used to verify the approximations employed in existing calculations of $\Delta\beta$. Moreno *et.al.* [9], for example, have calculated the Higgs profile of the bubble in the light stop scenario. They performed the calculation at the temperature we have called T_N, and also at $T_N + 0.4GeV$ and $T_N - 0.4GeV$, and the variation they obtained of $\Delta\beta$ along the bubble wall is very similar among these temperatures. Translating that temperature interval to the variable ε by $\Delta\varepsilon \simeq \Delta T/(T_c - T_0)$, where $\Delta T = 0.8GeV$ and $T_c - T_0 \simeq 3GeV$, gives $\Delta\varepsilon \simeq 0.2$. So the conclusion is that the parameter $\Delta\beta$ does not change significantly in an ample interval around ε_N, which, according to our results, includes the possible values of ε_t.

6 Conclusions and discussion

It is well know that phase transition dynamics plays an important role in electroweak baryogenesis. Although the production of the baryonic asymmetry of the Universe at the electroweak phase transition is an exciting possibility, it is clear that a complete picture of the phase transition is needed to check quantitatively this possibility. This includes the detailed investigation of the evolution of bubbles, as well as the accurate calculation of the temperature of the transition. In this paper we have investigated both of this problems, which are certainly related with each other.

We have determined the upper and lower temperature limits $T_{\max}$ and $T_{\min}$ inside the interval $T_0 - T_c$, between which the phase transition must take place regardless of the velocity of expansion of bubbles. Our main conclusion in this respect is that, for the electroweak phase transition, the lower bound on T_t avoids the possibility that the phase transition occurs at a temperature near T_0. This is good for baryogenesis, since in such a case the transition would proceed by an almost homogeneous growing of the Higgs field, what would lead to the generation of a smaller baryon abundance.

When the evolution of the bubble wall is included, the temperature of the phase transition varies between the limits $T_{\max}$ and $T_{\min}$ as the friction parameter η goes from 0 to ∞. However, it turns out that, due to the slow decreasing of temperature with time, the temperature T_t stays close to $T_{\max}$ for not extremely high values of η. According to our numerical computations, for likely values of the viscosity of the plasma the temperature of the electroweak phase transition is given by $S_3(T_t)/T_t \lesssim 90$.

On the other hand, the values of the wall thickness $l_w(T)$ and wall velocity $v_w(T)$ are rather insensitive to temperature in the range $T_{\min} - T_{\max}$, so they depend weakly on the actual temperature of the phase transition. Regarding the Higgs mean value $v(T)$, although baryogenesis is very sensitive to this parameter, and hence the uncertainty between $T_{\min}$ and $T_{\max}$ would still be considerable, the result that the phase transition takes place near $T_{\max}$ eliminates this uncertainty. Furthermore, the temperature $T_{\max}$ is in general close to that of the onset of nucleation. Hence we conclude that $l_w(T_t)$, $v_w(T_t)$, and $v(T_t)$, which are relevant parameters for baryogenesis, do not change significantly from those obtained with the usual estimation of the temperature of the transition, i.e., with the condition $S_3(T)/T \sim 135$. We have also shown that the same applies to other quantities, which we have not computed, such as the parameter $\Delta\beta$, which is relevant for electroweak baryogenesis in the context of the MSSM.

Regarding further development of this analysis, a detailed investigation of the effect of reheating due to the latent heat released by the expanding

bubbles would be necessary [31]. As we have discussed in section 4, such an investigation would be especially important in the case of the MSSM, where the main consequence of this effect would be to prevent the wall velocity to reach the value $\sim 10^{-3} - 10^{-2}$ that is needed for a satisfactory result of electroweak baryogenesis.

Acknowledgments

I would like to thank Prof. Luis Masperi for helpful comments. Part of this work was done with the support of a fellowship of the Consejo Nacional de Investigaciones Científicas y Técnicas, Argentina.

A The shape of bubbles

In this appendix we give some interesting details of the calculation of the bubble radius, the wall width, and the value of the Higgs field inside the bubble at the moment of formation.

The shape of the bubble is given by Eq. (10) with potential (2),

$$\frac{d^2\phi}{dr^2} + \frac{2}{r}\frac{d\phi}{dr} = 2D\left(T^2 - T_0^2\right)\phi - 3ET\phi^2 + \lambda\phi^3 \ . \tag{33}$$

Following Dine et al. [8], we define $\phi = \left[D\left(T^2 - T_0^2\right)/\left(ET\right)\right]\Phi$ and $r = R/\sqrt{2D\left(T^2 - T_0^2\right)}$, so that Eq. (33) becomes

$$\frac{d^2\Phi}{dR^2} + \frac{2}{R}\frac{d\Phi}{dR} = \Phi - \frac{3}{2}\Phi^2 + \frac{1}{2}\alpha\Phi^3 \ , \tag{34}$$

with $\alpha = \lambda D\left(T^2 - T_0^2\right)/\left(ET\right)^2$. We have solved numerically this equation with the usual overshooting-undershooting method, to obtain the configuration $\Phi\left(R\right)$ for different values of α. The graphics of Fig. 2 for ϕ/T as a function of the dimensionless radius Tr are then given by

$$\frac{\phi\left(T\right)}{T} = \frac{E\alpha}{\lambda}\Phi\left(\sqrt{\frac{2E^2\alpha}{\lambda}}Tr\right) \ . \tag{35}$$

The expression (11) for $S_3\left(T\right)/T$ is then obtained by an appropriate integration of the solution over $d^3X = 4\pi R^2 dR$.

We define the radius $R_0\left(\alpha\right)$ of the configuration as that at which $\Phi\left(R\right)$ falls to $\Phi_0/2$, where $\Phi_0\left(\alpha\right) = \Phi\left(R = 0\right)$. Similarly, we calculate the radii R_1 and R_2 corresponding to $0.9\Phi_0$ and $0.1\Phi_0$ respectively, and define the wall

width as $L_w = R_2 - R_1$. This quantities are related to the physical radius r_0 and width l_w of Fig. 1 by

$$Tr_0 = \frac{\sqrt{\lambda/2}}{E}\frac{1}{\sqrt{\alpha}}R_0(\alpha) \ , \quad Tl_w = \frac{\sqrt{\lambda/2}}{E}\frac{1}{\sqrt{\alpha}}L_w(\alpha) \ . \tag{36}$$

The value of the field inside the bubble, plotted in Fig. 3, is defined as $\phi_0 = \phi(r=0)$ and is related to the dimensionless Φ_0 by

$$\frac{\phi_0(T)}{T} = \frac{E}{\lambda}\alpha\Phi_0(\alpha) \ , \tag{37}$$

to be compared with the minimum $v(T)$ of the potential, given by

$$\frac{v(T)}{T} = \frac{E}{\lambda}p(\alpha) \ . \tag{38}$$

The divergence of r_0 and l_w at $\alpha = 0$ is apparent in Eq. (36). The divergence of r_0 at $\alpha = 1$, instead, is hidden in the function $R_0(\alpha)$. The wall width is finite at $\alpha = 1$, but due to the divergence of the radius the shape of the bubble wall cannot be calculated using the numerical method. Interestingly, in this limit L_w can be obtained analytically, what is useful to check that the numerical curve goes to the right limit for $\alpha \to 1$: Since $R_0 \to \infty$ the second term disappears from Eq. (34). Then multiplying by $\frac{d\Phi}{dR}$ and integrating over dR gives for $\alpha = 1$

$$\frac{d\Phi}{dR} = -\Phi\left(1 - \frac{\Phi}{2}\right) \tag{39}$$

Integrating again across the wall we obtain

$$L_w = \ln\left(\frac{\Phi - 2}{\Phi}\right)\Bigg|_{0.9\Phi_0}^{0.1\Phi_0} \ . \tag{40}$$

Similarly we can see that $\Phi(R)$ goes from 2 to 0 across the wall, so in this case $\Phi_0 = 2$, and Eq. (40) gives $L_w = 2\ln 9$. We can then verify that in Fig. 1, with $\lambda = 2E$ and $E = 0.06$, the wall width has the correct value at $\varepsilon = 0$.

References

[1] A. G. Cohen, D. B. Kaplan and A. E. Nelson, Annu. Rev. Nucl. Part. Sci. **43**, 27 (1993); M. Trodden, hep-ph/9803479; A. Riotto, hep-ph/9807454; A. Riotto and M. Trodden, Annu. Rev. Nucl. Part. Sci. **49**, 35 (1999).

[2] A. E. Nelson, D. B. Kaplan and A. G. Cohen, Nucl. Phys. **B373**, 453 (1992); M. Joyce, T. Prokopec and N. Turok, Phys. Lett. **B338**, 269 (1994); J. M. Kline, Pramana J. Phys. **54**, 1 (2000).

[3] A. Heckler, Phys. Rev. **D51**, 405 (1995).

[4] J. M. Cline and K. Kainulainen, hep-ph/0002272.

[5] A. G. Cohen, D. B. Kaplan and A. E. Nelson, Nucl. Phys. **B349**, 727 (1991).

[6] M. Joyce, T. Prokopec and N. Turok, Phys. Rev. Lett **75**, 1695 (1995); Erratum-ibid.**75**, 3375 (1995); Phys. Rev. **D53**, 2958 (1996).

[7] J. M. Cline and G. Moore, Phys. Rev. Lett **81**, 3315 (1998).

[8] M. Dine, R. Leigh, P. Huet, A. Linde and D. Linde, Phys. Rev. **D46**, 550 (1992).

[9] J. M. Moreno, M. Quirós and M. Seco, Nucl. Phys. **B526**, 489 (1998).

[10] M. Shaposhnikov, JETP Lett. **44**, 465 (1986); Nucl. Phys. **B287**, 754 (1987); Nucl. Phys. **B299**, 797 (1988).

[11] W. Buchmuller and Z. Fodor, Phys. Lett. **B331**, 124 (1994); W. Buchmuller and O. Philipsen, Nucl. Phys. **B443**, 47 (1995); K. Kajantie, M. Laine, K. Rummukainen and M. Shaposhnikov, Phys. Rev. Lett **77**; 2887 (1996); F. Csikor, Z. Fodor and J. Heitger, Phys. Rev. Lett **82**, 21 (1999).

[12] M. Carena, M. Quirós and C. Wagner, Nucl. Phys. **B254**, 3 (1998).

[13] G. Anderson and L. Hall, Phys. Rev. **D45**, 2685 (1992).

[14] J. R. Espinoza, M. Quirós and F. Zwirner, Phys. Lett. **B307**, 106 (1993).

[15] M. Carena, M. Quirós, A. Riotto, J. Vilja and C. Wagner, Nucl. Phys. **B503**, 387 (1997); M. Carena, M. Quirós and C. Wagner, Phys. Lett. **B380**, 81 (1996).

[16] L. McLerran, M. Shaposhnikov, N. Turok and M. Voloshin, Phys. Lett. **B256**, 451 (1991).

[17] A. D. Linde, Phys. Lett. **B70**, 306 (1977); **B100**, 37 (1981); Nucl. Phys. **B216**, 421 (1983).

[18] R. Fiore, A. Tiesi, L. Masperi and A. Mégevand, Mod. Phys. Lett. **A14**, 407 (1999).

[19] N. Turok, Phys. Rev. Lett **68**, 1803 (1992); B. Liu, L. McLerran and N. Turok, Phys. Rev. **D46**, 2668 (1992).

[20] S. Y. Khlebnikov, Phys. Rev. **D46**, 3223 (1992); P. Arnold, Phys. Rev. **D48**, 1539 (1993); G. D. Moore and T. Prokopek, Phys. Rev. **D52**, 7182 (1995).

[21] J. Ignatius, K. Kajantie, H. Kurki-Suonio and M. Laine, Phys. Rev. **D49**, 3854 (1994).

[22] K. Enqvist, J. Ignatius, K. Kajantie and K. Rummukainen, Phys. Rev. **D45**, 3415 (1992); H. Kurki-Suonio and M. Laine, Phys. Rev. **D51**, 5431 (1995); P. Huet, K. Kajantie, R. Leigh, B. Liu and L. Mclerran, Phys. Rev. **D48**, 2477 (1993).

[23] M. S. Turner and L. M. Widrow, Phys. Rev. **D37**, 2743 (1988); B. Ratra, Ap. J. **391**, L1 (1992); A.-C. Davis and K. Dimopoulos, Phys. Rev. **D55**, 7398 (1997); M. Joyce and M. Shaposhnikov, Phys. Rev. Lett**79**, 1193 (1997).

[24] J. Ahonen and K. Enqvist, Phys.Rev. **D57**, 664 (1998); G. Sigl, A. V. Olinto and K. Jedamzik, Phys.Rev. **D55**, 4582 (1997); G. Baym, D. Bödeker and L. McLerran, Phys. Rev. **D53**, 662 (1996); T. Vachaspati, Phys. Lett. **B265**, 258 (1991).

[25] M. Giovannini and M. Shaposhnikov, Phys. Rev. **D57**, 2186 (1998); P. Elmfors, K. Enqvist and K. Kainulainen, Phys. Lett. **B440**, 269 (1998); K. Kajantie, M. Laine, J. Peisa, K. Rummukainen and M. Shaposhnikov, Nucl. Phys. **B544**, 357 (1999).

[26] G. D. Moore, hep-ph/0001274.

[27] G. D. Moore and N. Turok, Phys. Rev. **D55**, 6538 (1997).

[28] P. John and M. G. Schmidt, hep-ph/0002050.

[29] A. H. Guth and E. J. Weinberg, Phys. Rev. **D23**, 876 (1981).

[30] P. John, Phys. Lett. **B452**, 221 (1999).

[31] A. Mégevand, work in progress.